Copyright © 2010 American Scientific Publishers
All rights reserved
Printed in the United States of America

Journal of
Nanoscience and Nanotechnology
Vol. 10, 1846–1851, 2010

A Facile Approach to Synthesize Alumina Nanostructures at Room Temperature

Xuehua Wang*, Chengyong Li, Lianjiao Ma, and Hong Cao

School of Materials Science and Engineering, Wuhan Institute of Technology, Wuhan 430073, China

Alumina nanostructures, nanowires, and semicolumn nanotubes with high aspect ratios were synthesized by the chemical etching of porous alumina membranes (PAMs) in phosphoric acid solution. The morphology and structure of alumina nanostructures were analyzed by scanning electron microscopy (SEM), energy dispersive spectrum (EDS), and X-ray diffraction (XRD), respectively. The results showed that the typical features of highly flexible nanostructures were around 20–40 nm in diameter and around 100 μm in length. EDS analysis indicated that the nanostructures were constructed by aluminum oxide. The crystalline structure of the alumina nanostructures was amorphous, which was in accordance with that of the PAMs. Furthermore, the morphology of the PAMs was characterized in detail by atomic force microscope (AFM) and SEM. On the basis of AFM and SEM observations, a possible formation mechanism of alumina nanostructures was discussed, and the inhomogeneous dissolution between the triple points and the side walls was considered to be the essential factor deciding the formation of nanostructures.

Delivered by Ingenta to:
The Chinese University of Hong Kong
IP: 137.189.42.254
Tue, 22 Jun 2010 03:30:21

Keywords: Nanostructures, Porous Alumina Membrane, Chemical Etching.

1. INTRODUCTION

The potential applications of one-dimensional nanostructured materials have attracted great attention over the past decade due to their particular dielectric and optical properties.[1–7] Alumina nanowires (ANWs) have high specific surface area, adsorption capacity, and excellent thermal and chemical stability and can be used for carriers of catalysts,[8] water purification filters,[9] and reinforcement of ceramic matrixes and metal-based composites.[10] Also, alumina nanotubes (ANTs) have many good aspects, such as flexibility[11] and important dielectric properties.[12] From these application viewpoints, ANWs and ANTs would be a potential nanocable for use in nanodevices.

Single-crystal Al_2O_3 fibers were first produced at Lawrence Berkeley Laboratory in 1996 using a basal sapphire (single crystal) substrate.[13] ANWs have recently been prepared by vapor-liquid-solid growth,[14] hydrothermal synthesis,[15,16] arc-plasma,[17] and high-temperature oxidization;[18] however, other methods, such as chemical etching porous alumina membranes (PAMs) in NaOH solutions to get ANWs or ANTs, were also reported by Han and Xu.[19,20] In this work, we report a convenient and inexpensive way to produce a high yield of ANWs and ANTs by etching PAMs in phosphoric acid solution at room temperature. The detailed formation process of ANWs and ANTs have been investigated by scanning electron microscopy (SEM), which gives more insight into the formation mechanism of ANWs and ANTs from the PAMs. Our observation revealed that the formation mechanism of ANWs and ANTs could be explained by the different etching rates among the side walls and the triple points caused by the hexagonal distribution of pores in the PAMs.

2. EXPERIMENTAL DETAILS

The PAMs used in this work were prepared via a two step aluminum oxidation process reported by Masuda et al.[21] High-purity (99.999%) aluminum foils were used as the basal materials. After being degreased in acetone and annealed at 500 °C for 7 h in a vacuum of about 1×10^{-1} Pa, the aluminum foils were electrochemically polished in a mixture of perchloric acid and ethanol (1:9 in volume) for 10 min under the constant voltage of 20 V at 0 °C. Then, the aluminum foils were rinsed in ethanol and distilled water several times. The anodization process was performed in 0.4 M oxalic acid at 20 °C under a constant voltage of 50 V for 30 min. After the first anodization, the PAMs were etched in a mixture of aqueous solution of phosphoric acid (5 wt%) and chromic acid (1.8 wt%) at 60 °C to remove the irregular oxide layer formed in the

*Author to whom correspondence should be addressed.

 1533-4880/2010/10/1846/006 doi:10.1166/jnn.2010.2117

first anodization. Then, the subsequent anodization under the same conditions as that in the first anodization was implemented for 4 h. The sample was immersed into a saturated $HgCl_2$ solution in order to dissolve the Al layer and obtain PAMs without the Al substrate. The separated PAMs were rinsed in deionized water several times. Samples (sized 10×10 mm) cut from the same PAMs with parallel nanochannels were etched with 5 wt% phosphoric acid solution for various periods of time at room temperature. Then, the samples were rinsed in deionized water and absolute ethanol several times in turn. By controlling the etching time, ANWs and ANTs were obtained.

The details and surface characteristics of alumina nanostructures and PAMs were characterized by SEM (model Philips SIRION 200, Philips, Holland) and atomic force microscopy (AFM, model CSPM4000, Shanghai, China). The crystalline structure of alumina nanostructures and PAMs was analyzed by X-ray diffraction (XRD, model XD-5A) with accelerating voltage of 20 kV and electric current of 30 mA applied.

Delivered by Inge
The Chinese University
IP : 137.189.42
Tue, 22 Jun 2010 0

3. RESULTS AND DISCUSSION

Figure 1 shows the SEM images of the surface view of PAM after the second anodization at 50 V in 0.4 M oxalic acid solution with a temperature of 20 °C. A well-ordered array of nanopores is observed. The diameter of the pores is in the order of 100 nm. The pore density can be as high as 1.0×10^{10} per square centimeter. The top surface morphology of PAM obtained in our experiments is shown in Figure 1(a). Apparently, each cell has a honeycomb structure, and the cell arrangement is fairly ordered. Figure 1(b) depicts a cross-section view of the PAM with pores parallel to each other and perpendicular to the surface of the membrane. Figure 1(c) shows an AFM image of the top surface of the PAM. The opening of each pore is not flat. The configuration of the PAM can be thought of as a pore surrounded by triple points. A concave shape where honeycombed cells exist can be observed between two neighboring protrusions. Samples (sized 10×10 mm) cut from the same PAMs after the second oxidation were immersed in 5 wt% phosphoric acid solution for 60 min. We found that in certain etching periods, a high yield of ANWs and ANTs can be observed in Figure 2. In contrast to conventional bulk alumina ceramics, ANTs and ANWs are highly flexible, as shown in Figure 2(a). Some can be sufficiently flexible to form camber, as labeled by the red arrowhead. Figure 2(a) shows that the shape of ANWs is fairly fine, with a slenderness ratio of about 5,000. The length of the ANWs is on the order of 100 μm at least, and the diameter is about 20 nm. A single ANW can be observed, as identified by *K* in Figure 2(b). The diameter is about 20 nm, and one end is thinner than the other. The reason is that the etching rate of the top surface is faster than the bottom due to the different hydrogen ion concentration between the

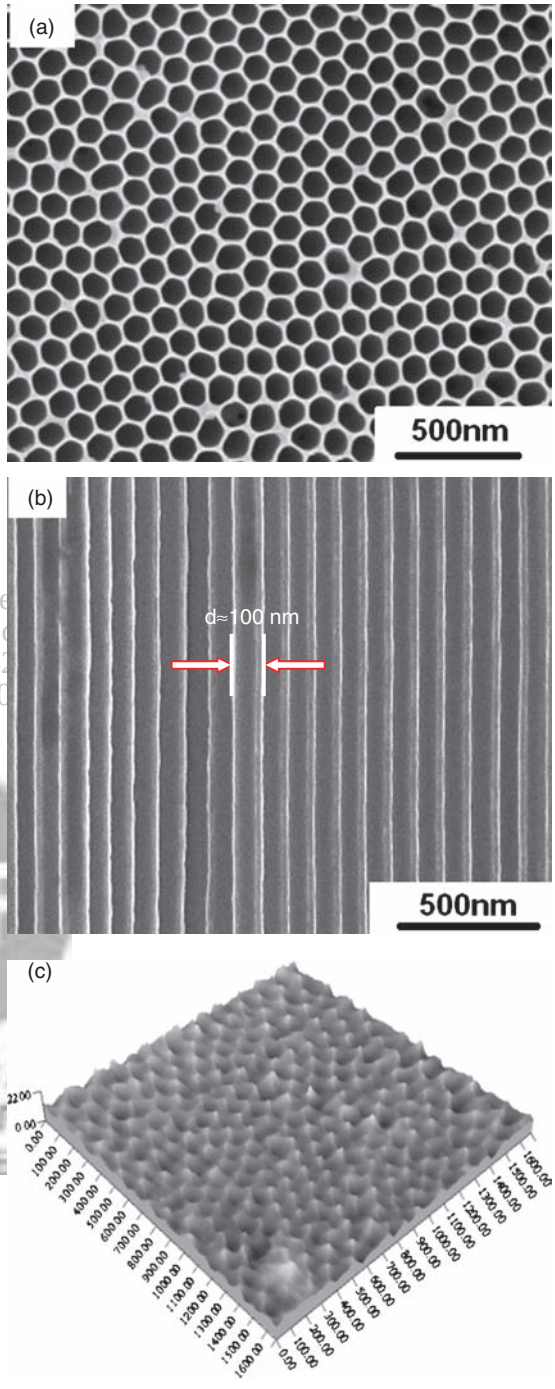

Fig. 1. Images of anodic alumina membrane after the second anodization at 50 V in 0.4 M $H_2C_2O_4$ at 20 °C and pore-widening for 40 min in 5 wt% phosphoric acid solution: (a) SEM image of the top surface, (b) SEM image of the cross-section surface, (c) AFM image of the top surface.

two ends. From Figure 2(b), a novel form of nanostructure-semicolumn nanotubes (so-called half-nanotubes) can be observed, as identified by *L*. Its diameter is about 35 nm, shown in Figure 2(b), which is bigger than the single ANW (*K*). They are transparent because the walls are so thin that an electron beam can pass through them.

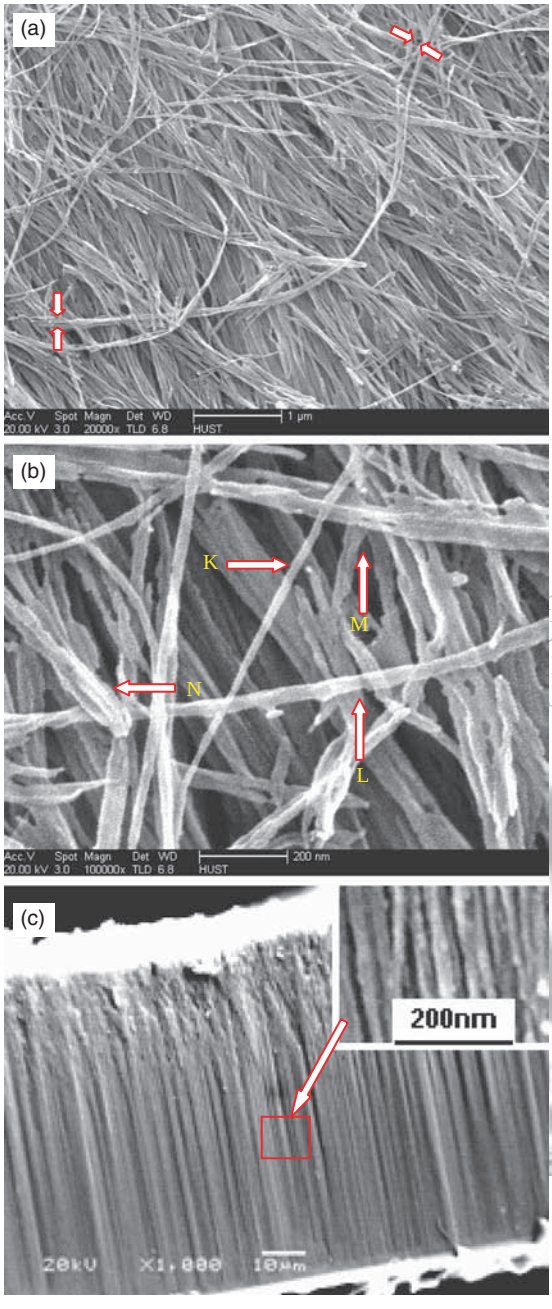

Fig. 2. SEM images of ANTs and ANWs prepared by etching PAM in 5 wt% phosphoric acid solution for 60 min: (a) top surface (×20,000), (b) top surface (×100,000), (c) cross-section surface (×1,000).

Conjugated half-nanotubes are abundant, as identified by *M*. Another novel multi-walled nanostructure of alumina in Figure 2(b) consisting of multi-half-nanotubes is identified by *N*. Figure 2(c) depicts a cross-section view of the alumina nanostructures showing that they have the same length as the PAM. From the inset of Figure 2(c), we can see the nanostructures are parallel to each other and perpendicular to the surface of the membrane.

Figure 3 is an energy dispersive spectrum (EDS) taken from the ANTs and ANWs. EDS analysis indicates that the

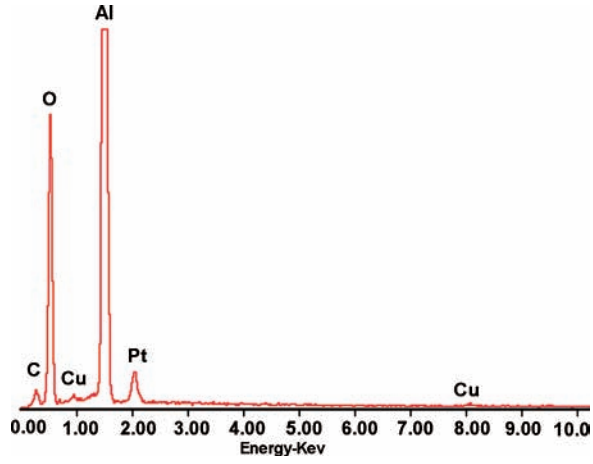

Fig. 3. EDS spectrum of the alumina nanostructures.

alumina nanostructure is mainly composed of the elements Al and O. The atom ratio of Al and O analyzed from the EDS data is 32.36% and 47.46% separately. The ratio of Al:O is 0.68, according to the stoichiometry of Al_2O_3, which is consistent with that of the PAMs. The Pt peak comes from the evaporated Pt for the SEM observation. The Cu peaks come from Cu electrode in the process of anodic oxidation. The *P* peak comes from phosphoric acid in the etching process.

Two curves in Figure 4 correspond to the XRD spectra of sample PAMs and alumina nanostructures. The broad peak around 27° indicates that alumina nanostructures are amorphous which is consistent with PAMs.

Figure 5 shows the SEM images of the alumina nanostructures after the PAMs were etched in 5 wt.% phosphoric acid solution for different times. Figure 5(a) shows an SEM image of the surface of the PAM without etching. The pore diameter is on the order of 50 nm, with the thickness of the wall about 60 nm. The inset of Figure 5(a) clearly shows that the back of the PAM is absolutely

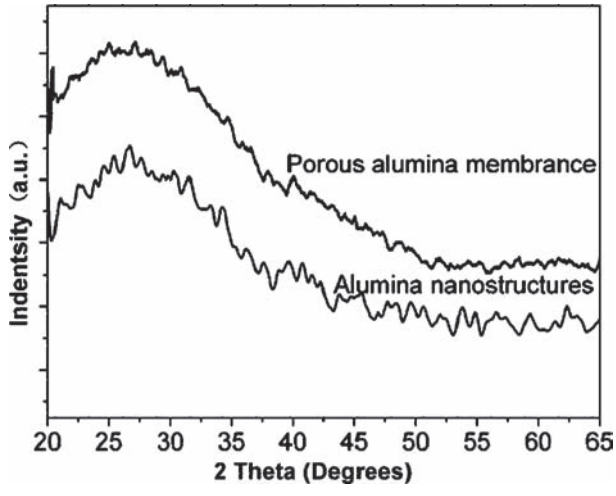

Fig. 4. XRD patterns of PAMs and ANWs.

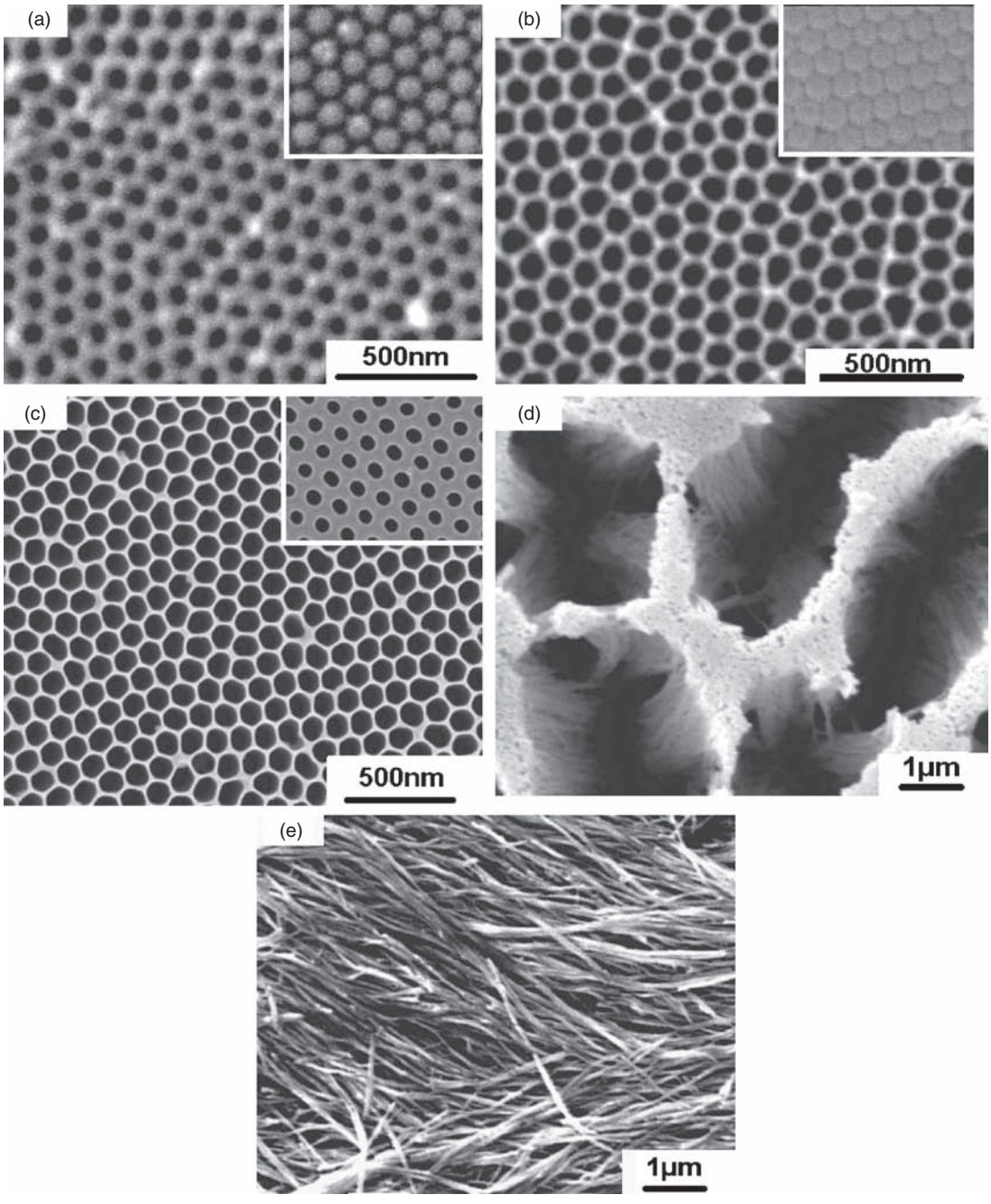

Fig. 5. SEM images of PAM film after etching in 5 wt% phosphoric acid solution for different times: (a) 0 min, (b) 30 min, (c) 40 min, (d) 50 min, and (e) 60 min.

closed. Figure 5(b) shows an SEM image of the surface of the PAM etched in phosphoric acid solution for 30 min. The pore diameter is about 70 nm, and the thickness of the pore wall is about 40 nm. The inset of Figure 5(b) clearly shows that the back of the PAM is partially dissolved. Figure 5(c) shows an SEM image of the surface of PAM as etched for 40 min, which is depicted in Figure 1. Usually a solution can enter small pores through the capillary effect. If air exists in the pores, however, it could hinder the complete filling of the pores. This situation is likely the case in our geometry, as one side of the membrane is coated with a barrier layer, effectively closing off the pores on that side. Subsequently, this means that the solution could reach only a certain depth within the pore through its open end at the beginning. In this case, the pore size of the top surface is wider than the bottom surface. The SEM image of the top surface shows a totally different pore size from the bottom surface in Figure 5(c). The pore diameter of the top surface is about 100 nm, and the pore diameter of the bottom surface is about 60 nm.

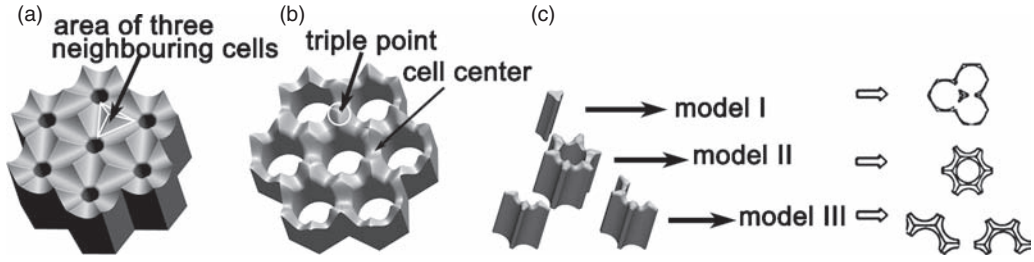

Fig. 6. Schematic illustration of the formation mechanism of the alumina nanostructures from PAM: (a) the original structure of PAM with a communal area of every three cells, (b) the expanded pores with triple points after etching, and (c) three models of the alumina nanostructures.

On the basis of Figures 5(a, b, and c), it is can be seen that both the walls of pores and barrier layers are dissolved gradually. At the same time, the pore diameter is increased as etching time is increased. The SEM image in Figure 5(d) shows the top view of naturally formed alumina nanostructure bundles that are composed of a high yield of ANWs and ANTs, as etching time is 50 min. The remnant walls lose their support from the neighboring thin walls. Consequently, they tend to lean against others formed nearby, so as to form natural bundles. The alumina nanostructures are horrent and parallel to each other. The presence of these naturally formed nanostructure bundles indicate that they are created in the natural course of etching as the phosphoric acid solution penetrates in a top to bottom direction. When the etching solution reacts with the PAMs further, the nanobundles collapse and transform into absolute nanowires and nanotubes, as shown in Figure 5(e). As a result, to get uniform nanostructures, it is important to control the etch time in phosphoric acid solution, which is usually about 50 min.

We propose the following formation mechanism of alumina nanostructrues. The PAMs consist of perfect hexagonal cells, and a communal area exists among three neighboring pores, as indicated in Figure 6(a). The pore size is broadened, and the thickness of the wall is reduced with etching in the phosphoric acid solution as described in Figure 6(b). With increased etching time, the cell center will be etched faster than other walls, as depicted in Figure 6(b). For a specific area, if the three outer nanotubes are broken simultaneously, we can then obtain a single intact nanowire in every triple point; we call this model I. For a specific nanotube, if all the breaking spots are exactly located at its six cell centers, then it can be separated from the membrane with six half-walls. Admittedly, this is an ideal breaking fashion and might happen incidentally; we call this model II. For most nanotubes, not all the breaking spots are located at the six cell centers. Some neighboring nanotubes have to be sacrificed in order to obtain one nanotube. Therefore, the residual walls from neighboring broken nanotubes are attached to it; we call this model III. Schematic diagrams of the three models are plotted in Figure 6(c). Practically, the three models will appear simultaneously when the PAM is subjected to etching in phosphoric acid solution. However, model III is evidently a predominant breaking mode, as shown in Figure 6(c). We can see that most cells are broken across the thinnest common walls of adjacent tubes. This model also determines the morphology of the final nanostructures. In Figure 2(b), the situation for model III is visible (shown by *L* and *M*). Since model II is a relatively perfect cleavage fashion, as shown by *N* in Figure 2(b), it was often difficult to observe in our current experiments.

Perhaps, most would take for granted the belief that the breaking spots of the cells would be located at the centers of the cell walls.[19, 20] According to this inference, all of the broken cells would have exhibited wirelike configurations; however, no specific breaking spots exist. In Figure 2(b), the broken cells display various configurations with some cells exhibiting a semicolumn and multi-semicolumn configuration. Some cells only lost a small part of the wall, while some cells were almost completely damaged. We speculate that the cause responsible for irregular breaking spots may be that the diffusing rate of the aqueous solution of phosphoric acid is different in the pores.

Delivered by Ingenta to:
The Chinese University of Hong Kong
IP: 137.189.45.34
Tue, 22 Jun 2010 03:36:21

4. CONCLUSIONS

A mass of amorphous alumina nanostructures can be synthesized by the chemical etching of PAMs in phosphoric acid solution. EDS analysis indicates that the amorphous nanostructures are constructed of aluminum oxide. The diameter of alumina nanostructures is about 35 nm, and the length is about 100 μm. The tubular structures are collections of opened side walls of nanopores, which might be caused by the dissolution and collapse of pore walls. We studied the dissolution process of PAMs in phosphoric acid solution and found that the different etching rates among the triple points and the side walls should be responsible for the formation of alumina nanostructures. We demonstrated that a high output of alumina nanostructures can be achieved by controlling the etching time.

Acknowledgments: This work was supported by the Wuhan Chenguang Plan Foundation in Hubei Prov., China through Grant No. 20065004116-35 to one of the authors (Xuehua Wang). The provided support is gratefully acknowledged.

References and Notes

1. S. Iijima, *Nature (London)* 353, 56 **(1991)**.
2. S. Iijima and T. Ichihashi, *Nature (London)* 363, 603 **(1993)**.
3. N. Hamada, S. Sawada, and Oshiyama, *Phys. Rev. Lett.* 68, 1579 **(1992)**.
4. J. C. Adenilson and J. C. Alexandre, *Physica E* 40, 449 **(2007)**.
5. D. R. Cornejo and E. Padrón-Hernández, *J. Magn. Magn. Mater.* 316, e48 **(2007)**.
6. W. Chen, *J. Nanosci. Nanotechnol.* 8, 1019 **(2008)**.
7. W. B. Bu and J. L. Shi, *J. Nanosci. Nanotechnol.* 8, 1266 **(2008)**.
8. A. Kolmakov and M. Moskovits, *Annu. Rev. Mater. Res.* 34, 151 **(2004)**.
9. F. Tepper, M. Lerner, and D. Ginley, *Am. Ceram. Soc. Bull.* 80, 57 **(2001)**.
10. T. L. Dragone and W. D. Nie, *Acta Metall. Mater.* 40, 2781 **(1992)**.
11. Y. F. Mei, X. L. Wu, X. F. Shao, G. G. Siu, and X. M. Bao, *Europhys. Lett.* 62, 595 **(2003)**.
12. Y. C. Wang, I. C. Leu, and M. H. Hon, *J. Appl. Phys.* 95, 1444 **(2004)**.
13. Lawrence Berkeley Laboratory (LBL) internal report. **(1996)**.
14. V. Valcarcel, A. Souto, and F. Guitian, *Adv. Mater.* 10, 138 **(1998)**.
15. F. Tepper, L. Kaledin, and C. Hartmann, *J. Water Conditioning Purification* 47, 55 **(2005)**.
16. H. C. Lee, H. J. Kim, and S. H. Chung, *J. Am. Chem. Soc.* 125, 2882 **(2003)**.
17. C. Arnoult, X. Devauxt, and H. Rinnert, *J. Mater. Sci. Technol.* 22, 127 **(2006)**.
18. C. C. Tang, S. S. Fan, and P. Li, *J. Cryst. Growth* 224, 117 **(2001)**.
19. J. K. Hana, J. Kima, and Y. C. Choi, *Physica E* 36, 140 **(2007)**.
20. X. J. Xu, G. T. Fei, and L. Q. Zhu, *Mater. Lett.* 60, 2331 **(2006)**.
21. H. Masuda and K. Fukuda, *Science* 268, 1466 **(1995)**.

Received: 26 November 2008. Accepted: 6 March 2009.

Delivered by Ingenta to:
The Chinese University of Hong Kong
IP : 137.189.42.34
Tue, 22 Jun 2010 03:36:21

ASP
AMERICAN
SCIENTIFIC
PUBLISHERS